Probing the Kinetic Mechanism and Coenzyme Specificity of Glutathione Reductase from the Cyanobacterium *Anabaena* PCC 7120 by Redesign of the Pyridine-Nucleotide-Binding Site†

U. Helena Danielson, Fanyi Jiang, Lars O. Hansson, and Bengt Mannervik*

Department of Biochemistry, Uppsala University, Biomedical Center, Box 576, S-751 23 Uppsala, Sweden

Received February 10, 1999; Revised Manuscript Received May 17, 1999

ABSTRACT: Glutathione reductase from the cyanobacterium *Anabaena* PCC 7120 contains a pyridine-nucleotide-binding motif differing from that of the enzyme from other sources and an insertion of 10 amino acid residues. Homology modeling was used to obtain a model of the enzyme structure. It revealed that in the *Anabaena* enzyme Lys^{203} replaces Arg, found to interact with the 2'-phosphate of NADP(H) in the enzyme from other sources, and that it has an extra loop near the entrance of the pyridine-nucleotide-binding site. The steady-state and preequilibrium kinetic properties were characterized for the wild-type enzyme, a K203R, and a loop deletion mutant. All enzyme forms had higher catalytic efficiency with NADPH than with NADH, although the difference was less than for glutathione reductase from other sources. The specificity was most pronounced in the formation of the charge-transfer complex between the pyridine nucleotide and oxidized enzyme-bound FAD, as compared to later steps in the reaction. Unexpectedly, by replacing Lys^{203} with Arg, the specificity for NADPH was diminished in the complete redox reaction. Ser^{174} appears to interact with the 2'-phosphate of NADPH and introduction of arginine instead of lysine, therefore, has little effect on the interaction with this coenzyme. However, the efficiency in forming the charge-transfer complex between the pyridine nucleotide and oxidized enzyme-bound FAD was increased in the K203R mutant using NADPH but not with NADH. The lack of affinity toward 2′,5′-ADP-Sepharose by the wild-type enzyme was not changed by replacing Lys^{203} with Arg but deletion of the loop resulted in an enzyme that bound to the immobilized ligand. Removal of the loop increased the efficiency of the enzyme in the reductive half-reaction with both pyridine-nucleotides as well as in the overall catalytic mechanism.

Glutathione reductase (EC 1.6.4.2) is a member of the pyridine-nucleotide disulfide oxidoreductase family of flavoenzymes (for a review, see ref *1*). The enzyme catalyzes the reduction of glutathione disulfide by using NADPH or NADH as a reducing agent.

$$GSSG + NADPH + H^+ \rightarrow 2\,GSH + NADP^+$$

The enzyme has been isolated, characterized, and sequenced from several different sources (*2*). The structure of glutathione reductase from human erythrocytes (*3*) and *Escherichia coli* (*4*) has been determined by X-ray crystallography, showing that the enzyme is a dimer with a redox-active disulfide and an FAD prosthetic group in each subunit.

The gene encoding glutathione reductase, *gor*, from *Anabaena* PCC 7120 has been isolated, the coding sequence cloned, and the protein heterologously expressed in a glutathione reductase-deficient *E. coli* strain (*5, 6*). Sequence analysis indicated that the enzyme might show different coenzyme specificity than glutathione reductase from other sources. In the *Anabaena* enzyme, the coenzyme fingerprint motif (amino acids 173−178) is GXGXXG, as normally found in NAD(H)-dependent enzymes (*7, 8*). In contrast, NADP(H)-dependent enzymes generally contain the motif GXGXXA, which is also the consensus sequence for glutathione reductases from most sources, consistent with its preference for NADPH. The first three residues in both fingerprint motifs, GXG, interact with the adenine, ribose, and pyrophosphate components of the pyridine nucleotide (*9*). In addition, NADP(H)-dependent enzymes have two arginines involved in binding of the 2′-phosphate of the coenzyme (Arg^{218} and Arg^{224} in human glutathione reductase) (*7*). The first arginine is present in the *Anabaena* enzyme (Arg^{197}), but the second one is replaced by lysine (Lys^{203}). NAD(H)-dependent enzymes lack these positively charged groups, but have a conserved acidic group in this region (*7*), not present in the *Anabaena* enzyme. It therefore appears that the coenzyme-binding motif in *Anabaena* should be regarded as a modified NADPH-binding motif rather than an NADH-binding motif. Preliminary kinetic studies (*6*) showed that the enzyme has a preference for NADPH, although it was found that activity was also obtained with NADH. However, these studies indicated that the *Anabaena* enzyme has lower affinity for NADPH than have the *E. coli* and human enzymes. Also, the *Anabaena* enzyme was unable to

† This study was supported by the Swedish Natural Science Research Council.

* To whom correspondence should be addressed. Phone: +46 18 471 45 39. Fax: +46 18 558431. E-mail: Bengt.Mannervik@biokem.uu.se.

10.1021/bi9903300 CCC: $18.00
Published on Web 07/02/1999

bind to 2′,5′-ADP−Sepharose 4B. This adsorbent is generally useful as an affinity matrix for purification of the enzyme (*10*−*12*), although the binding affinity varies among the enzymes from different sources.

To characterize the catalytic mechanism and the coenzyme specificity of *Anabaena* glutathione reductase, we modeled the three-dimensional structure of the enzyme. The unique structural features of the enzyme were used as a basis for redesign of the protein in order to analyze their importance for substrate binding and catalysis and to find if an enzyme with a higher catalytic efficiency could be obtained.

EXPERIMENTAL PROCEDURES

Structural Modeling. The structural model was built using Insight, Discover, and Homology software, version 2.3.0 (Molecular Simulations Inc, San Diego, CA). Glutathione reductase sequences from different species available in the EMBL and SWISS databases, and the *Anabaena* sequence deduced from the cloned DNA (*5*) were matched using multiple alignment (PileUp, GCG, Wisconsin). The coordinates of glutathione reductase from *E. coli* (Gre_Ecoli), supplied by Prof. Georg Schulz, University of Freiburg, Germany, and human (1gra) (*12*), obtained from the Protein Data Bank (*13*, *14*) were used to structurally align the enzymes.

Construction of Anabaena Glutathione Reductase Mutants. The plasmid containing the *Anabaena* PCC 7120 glutathione reductase gene (*5*) was used as a template in the overlap extension PCR described by Higuchi et al. (*15*) to create mutations. The point mutation (K203R) was introduced by using primer m1f (5′-GTGACAAAATTCTCAGAG-GTTTTGATG-3′) and its reverse primer m1r (5′-AAAC-CTCTGAGAATTTTGTCAC-3′). The deletion mutation (Δloop) was introduced by primer m2f (5′-GTTGTTGA-CAAAGGTCACATTGCAGT-3′) and its reverse primer m2r (5′-CTGCAATGTGACCTTTGTCAACAAC-3′). In addition, 5′ and 3′ glutathione reductase primers were used for mutagenesis PCR. The 5′ primer contains the first 14 codon sequence following the start codon: 5′-TCTAGAATTCAT-GACTTTTGACTACGACCTGTTTGTA ATTGGTGCTG-GTTCCGGTGGTTTGGC-3′. The nucleotide sequence is not identical to the wild-type glutathione reductase sequence, but the codons still specify the amino acids of the wild-type protein. The silent mutations were introduced to optimize protein expression (*6*). The 3′ primer contains the glutathione reductase 3′ terminal coding sequence and an additional six histidine codons before the stop codon: 5′-AGTC-GACAAGCTTATTAATGGTGATGGTGATGGT-GTCGCATAGTGACAAATTCCTCGGC-3′. The latter primers also contain flanking restriction enzyme sites that were used for recloning. The PCR was carried out with denaturation at 95 °C for 2 min, annealing at 58 °C for 2 min and elongation at 72 °C for 2 min for 33 cycles. The final PCR product of about 1.3 kb was cloned through *Eco*RI and *Sal*I cloning sites into the expression vector pGEM-Tac: the Tac promoter was inserted in front of the polylinker region of pGEM 3Zf(+) (*16*). The constructs pGTacGRWT (containing the wild-type glutathione reductase gene), pGTacGRM1 (the point mutant K203R), and pGTacGRM2 (the deletion mutant Δloop) were introduced into the glutathione reductase deficient *E. coli* strain SG5 for expression.

DNA Sequencing. The glutathione reductase gene in the pGEM-Tac vector was sequenced with Sequenase version 2.0 (United States Biochemical Corp) by the dideoxynucleotide termination method (*17*). Reactions were primed with the pUC/M13 forward primer, the pUC/M13 reverse primer, and oligonucleotides complementary to insert sequences, respectively. Oligonucleotides were custom synthesized by Operon Technologies Inc. (Alameda, CA).

Glutathione Reductase Expression and Purification. E. coli SG5 cells carrying either wild-type glutathione reductase or glutathione reductase mutants were grown to OD = 0.3 and induced by 0.4 mM IPTG. They were continuously cultured overnight at 37 °C. Cells from a 3 L culture were harvested by centrifugation at 5000*g* and resuspended in 80 mL of 0.1 M sodium phosphate (pH 7.0) and 1 mM EDTA (buffer A). The suspension was subjected to sonication for 3 × 20 s, and centrifuged at 25000*g* for 15 min. Solid ammonium sulfate was added to the supernatant to reach 30% saturation. The precipitate was collected by centrifugation at 25000*g* for 20 min and discarded. Solid ammonium sulfate was added again to the supernatant to give 60% saturation. After centrifugation, the pellet was dissolved in a minimal volume of 20 mM sodium phosphate (pH 7.0) and 0.5 M NaCl (buffer B) and dialyzed against the same buffer. The sample was then applied to a Ni(II)-IMAC column (4 × 8 cm) equilibrated with buffer B. Chelating Sepharose FF was purchased from Pharmacia Biotech, and the IMAC column was prepared according to the manufacturer's guidelines. The column was washed with buffer B, and the enzyme was eluted with a linear gradient of 0 to 300 mM imidazole in buffer B. The fractions containing glutathione reductase activity were pooled and concentrated by Millipore ultrafiltration (Millipore, Bedford, MA). The purity of the protein was detected by SDS−PAGE developed by silver staining (*18*). Glutathione reductase concentration was determined on the basis of an extinction coefficient of 11.3 mM^{-1} cm^{-1} at 462 nm (*19*) for the flavin. All enzyme variants contained a C-terminal hexa-histidine sequence in order to facilitate purification (*6*). No alteration of the kinetic properties of the enzyme caused by this modification has been detected.

Affinity for Immobilized 2′,5′-ADP-Sepharose. The affinity of purified wild-type and mutant forms of glutathione reductase for 2′,5′-ADP-Sepharose 4B (Pharmacia Biotech, Uppsala, Sweden) was determined by chromatography essentially as described by the manufacturer. Glutathione reductase from yeast (Boehringer-Mannheim) was used as a positive control. The column was equilibrated with 10 mM sodium phosphate, pH 7.3, and 0.15 M NaCl, and the enzyme was applied at a low flow rate (<0.5 mL/min). The column was subsequently washed with the same buffer, and bound enzyme was eluted with buffer containing 0.5 M KCl (*20*).

Steady-State Kinetics. The enzymatic reduction of GSSG[1] by NADPH (or NADH) was assayed at 30 °C, as previously described (*20*). Briefly, the rate of oxidation of NADPH at 30 °C in 0.1 M Na_2HPO_4/NaH_2PO_4, pH 7.0, and 1.2 mM GSSG was measured by monitoring the decrease in absorbance at 340 nm (ϵ_{340} = 6220 M^{-1} cm^{-1}). The concentration of NADH and NADPH was determined from their absorbance spectra using the same extinction coefficient. The

[1] Abbreviations: GSH, glutathione; GSSG, glutathione disulfide.

optimal pH values for the enzyme variants with the different coenzymes were determined using 200 μM NADPH or 240 μM NADH in 0.1 M sodium phosphate (pH 5.8, 7.0, and 8.0) or Tris-HCl (pH 9.3). The values of the apparent Michaelis constant (K_M) and the catalytic constant (k_{cat}) were determined from experimental steady-state kinetic data, from two parallel experiments. Data were analyzed by nonlinear regression using the Michaelis−Menten equation (GraphPad, GraphPad Software Inc) or when two substrates were varied using the rate equation for a ping−pong mechanism (Grafit, Erithacus Software Ltd., England). Constants are given with standard errors from nonlinear regression of two parallel experiments. The assays for NADPH were performed at pH 7.0, using 0.5−24 μM NADPH. NADH measurements were performed at both pH 7.0 and pH 8.0, using 15−720 μM NADH. The K_M for GSSG was determined using 50, 100, and 200 μM NADPH, at GSSG concentrations varying from 0.6 to 24 μM.

Steady-state kinetics at 5 °C were studied in a stopped-flow apparatus (Applied Photophysics, model SX.18MV, England) where a mixture of the two substrates was added to the enzyme. The velocity of the reaction was monitored at 340 nm. The initial concentration of NADPH used in subsequent calculations was determined from the absorbance at zero time. At least four replicates were used for determination of kinetic constants, providing standard errors in the nonlinear regression analysis.

Preequilibrium Kinetics. Preequilibrium kinetic experiments were performed using a stopped-flow spectrophotometer (see above), fitted with a photomultiplier tube and a 1 cm cell. All measurements were carried out in 0.1 M sodium phosphate pH 7.0 at 5 °C. The buffer of the enzyme stock solution was changed into sodium phosphate using a PD-10 column (Pharmacia Biotech, Sweden). Samples were deaerated in the storage syringes before mixing, and nitrogen was continuously blown over the entrances of the sample syringes, minimizing the presence of oxygen at the start of experiments. The experiments were conducted under pseudo-first-order conditions where the ratio of substrate to enzyme concentration was equal to or larger than 14:1. An average of 3−6 individual traces was fitted by different alternative equations using the Applied Photophysics software. Further analysis of kinetic data was carried out using GraphPad. The reductive half-reaction, where enzyme was mixed with either NADH or NADPH (no GSSG), was monitored at 460 and 525 nm.

The rate of reoxidation of NADH-reduced FAD at 25 °C by dissolved oxygen has been shown to be slow and not to have any significant effect on the observed rate (*21*). In our experiments with NADPH, no decrease in the absorbance at 525 nm (expected if reoxidation were to occur) was noticed during the time period of the experiments (data not shown).

RESULTS

Homology Modeling. As a basis for modeling of the three-dimensional structure of glutathione reductase from *Anabaena* PCC 7120, an alignment with nine amino acid sequences was performed, including such from organisms representing different evolutionary branches. The *Anabaena* sequence was found to be similar in its essential features to all glutathione reductase sequences, but it was not clearly more similar to one or the other of the human or *E. coli* sequences, the crystal structures of which are known. Both of these primary structures contained segments that matched the *Anabaena* sequence better than the alternative. They were therefore both used as references for model building. To have the best possible starting point for modeling, a structure-based alignment of the *E. coli* and the human sequences was used; this latter differs slightly from the original sequence alignment especially in regions where gaps are present.

The insert of 10 amino acids (no. 282−291), present only in the *Anabaena* sequence, could not be modeled accurately. It forms a loop near the entrance of the coenzyme-binding pocket (Figure 1). Despite several combined runs of molecular dynamics and energy minimization, a stable structure (energy minimum) was not obtained. The structure in Figure 1 shows the loop in the "open" position.

The overall fit of the *Anabaena* structure to the two glutathione reductase structures used as references was good, Figure 1. The root-mean-square (RMS) difference in the polypeptide backbone was 1.06 and 0.98 Å in relation to the *E. coli* and human proteins, respectively. The most obvious difference in the *Anabaena* structure as compared to the other two structures is the presence of the extended loop adjacent to the pyridine-nucleotide-binding site.

The initial structural sequence alignment was refined manually by overlaying the three structures so that the backbone of conserved residues in the region overlapped. Residues in similar positions were identified (Figure 2). Those that were aligned differently than predicted by either of the two initial sequence alignments were all found in regions where the different enzymes contained insertions or deletions. In addition, an extra loop found only in the human structure was modeled between amino acid residues Glu^{247} and Asp^{248} in the *Anabaena* sequence. The human loop is positioned close to the entrance of the coenzyme-binding site, like the *Anabaena* loop. However, it is placed at the opposite side of the coenzyme-binding cavity (Figure 1).

Nucleotide-Binding Sites. The binding of the prosthetic group FAD involves a characteristic sequence, GXGSGG, near the N-terminus of glutathione reductase. Comparison of this FAD-binding motif (*Anabaena* residues 11−16) of glutathione reductase from different sources shows a very high degree of conservation. In the *Anabaena* sequence, X is alanine, while it is glycine in both the human and *E. coli* sequences. The alanine is in contact with several other residues but does not appear to be in contact with FAD (Figure 3); it actually points away from the adenosine moiety of FAD. Alanine is commonly occurring in this position in glutathione reductase from other sources, and the presence of glycine or alanine appears to lack functional significance.

The pyridine-nucleotide-binding site in the *Anabaena* structure is slightly different from that of the human and *E. coli* structures. The characteristic NADPH-binding motif reads GSGYIG in the *Anabaena* sequence, amino acid residues 173−178. It differs from other glutathione reductase sequences in the second position (Ser^{174}), where the enzyme from other sources have glycine or alanine instead of serine. The *Anabaena* sequence also differs in the last position of the binding motif, where a glycine is present (Gly^{178}); glutathione reductase from other sources has alanine or serine in this position. The model shows that the hydroxyl group of the side chain of *Anabaena* Ser^{174} can be in close contact

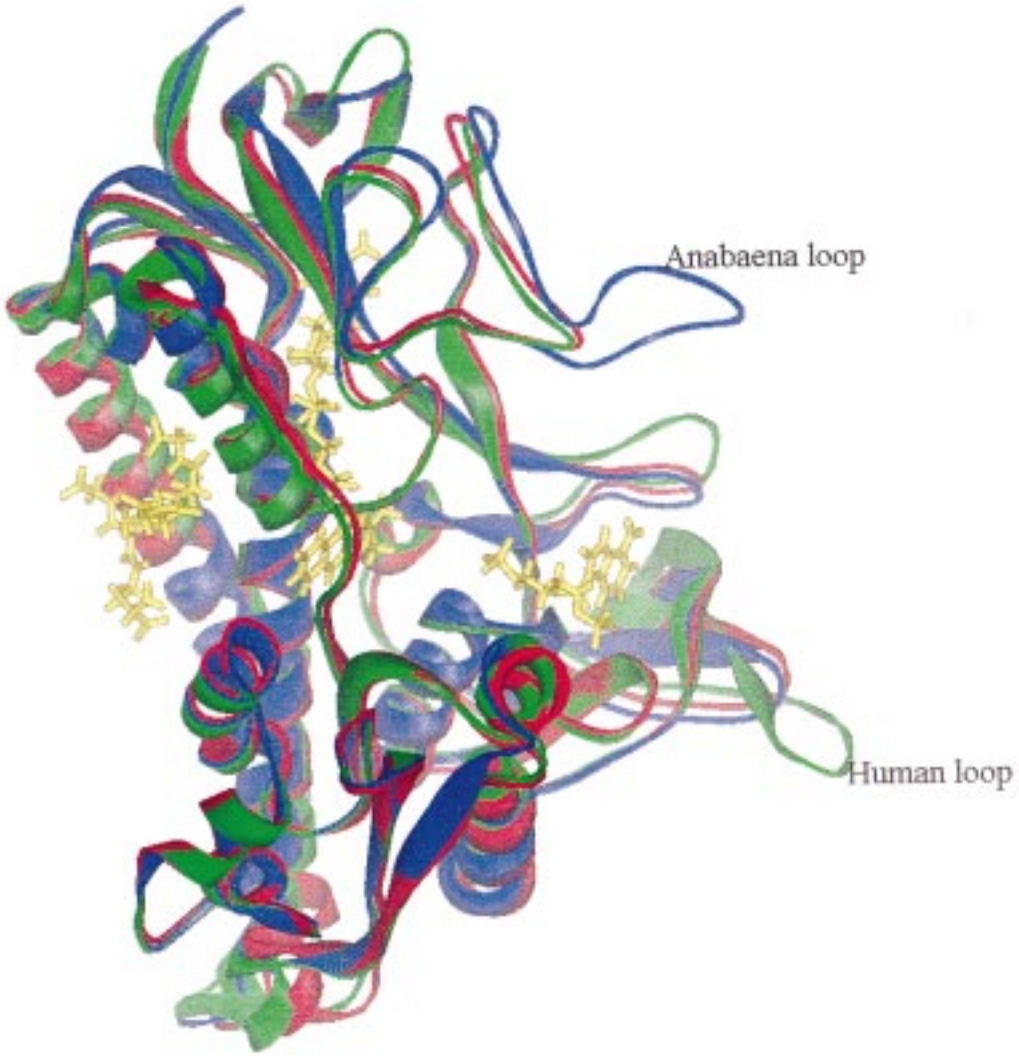

FIGURE 1: Modeled structure of *Anabaena* (blue) superpositioned on glutathione reductase structures of the human (green) (*12*) and *E. coli* (red) (*4*) enzymes determined by X-ray diffraction analysis. FAD, 2',5'-ADP and GSSG (all yellow) are from the human structure (*12*).

with the 2′-phosphate of NADPH (Figure 4), an interaction not possible in the other structures since they do not contain amino acids with side chains that form hydrogen bonds. Instead they have an arginine in position 203 that interacts with the 2′-phosphate of NADPH (Figure 4). In *Anabaena* glutathione reductase the residue in position 203 is a lysine, making the interaction between residue 203 and the 2′-phosphate of NADPH less favorable due to an increased distance. It therefore appears as if the substitution in position 174 is related to the substitution in position 203. A third residue, Arg^{197}, is also in close proximity to the 2′-phosphate of NADPH (Figure 4). It is conserved in all known glutathione reductase sequences, including that from *Anabaena*.

GSSG-Binding Site. Residues involved in the catalytic process at the GSSG-binding site were also examined. The redox-active disulfide formed by two Cys residues (numbers 42 and 47) is conserved both in the primary structure and in the three-dimensional model. His^{447}, which serves as an acid in the protonation of the glutathione thiolate produced from the GSSG (*22*−*24*), is conserved and occurs in a position suitable for such a role also in the *Anabaena* enzyme. On the other hand, the evolutionarily conserved tyrosine (residue 114 in the human enzyme) that assists in the mechanism by interacting with the sulfur atoms of GSSG, is replaced by His^{98} in an equivalent position in the primary structure and in the structural model of the *Anabaena* enzyme. It is reasonable to assume that His^{98} could serve a function similar to that proposed for the corresponding tyrosine in glutathione reductase from other species (*25*).

Construction and Expression of Mutant Enzymes. The glutathione reductase K203R and Δloop (Δ282−291/M292K/N293G/A294H) mutants were obtained by PCR-mediated oligonucleotide-directed mutagenesis as described in the Experimental Procedures. The deletion mutant was first designed as Δ282−291/M292G, where the loop residues were removed and the residue in position 292 was changed into glycine. The other two enzymes have lysine in this position, while the *Anabaena* has a methionine; glycine was taken as an alternative without side-chain functionality. However, attempts to express this mutant in *E. coli* were not successful (data not shown). The Δloop mutant was therefore redesigned with further mutations, introducing the conserved lysine and the succeeding glycine and histidine residues (present in the human enzyme). Both the K203R and the Δloop mutants were expressed in *E. coli* SG5, and subsequently purified by Ni(II)-IMAC. The yield of the K203R mutant of glutathione reductase was about 17 mg/L

```
ANABAE: MTFDYDLFVIGAGSGGLAASKRAASYGAKVAIAENDLVGGTCVIRGCVPK    50
HUMAN : >VASYDYLVIGGGSGGLASARRAAELGARAAVVESHKLGGTCVNVGCVPK    66
ECOLI : MTKHYDYIAIGGGSGGIASINRAAMYGQKCALIEAKELGGTCVNVGCVPK    50
                  FAD motif                          *S----S*

                                                          98
ANABAE: KLMVYGSHFPALF-EDAAGYGWQVGKAELNWEHFITSIDKEVRRLSQLHI    99
HUMAN : KVMWNTAVHSEFM-HDHADYGFPSCEGKFNWRVIKEKRDAYVSRLNAIYQ   115
ECOLI : KVMWHAAQIREAIHMYGPDYGFDTTINKFNWETLIASRTAYIDRIHTSYE   100

ANABAE: SFLEKAGVELISGRATLV-DNH-TVEVGERKFTADKILIAVGGRPIKPE-   146
HUMAN : NNLTKSHIEIIRGHAAFTSDPKPTIEVSGKKYTAPHILIATGGMPSTPHE   165
ECOLI : NVLGKNNVDVIKGFARFV-DAK-TLEVNGETITADHILIATGGRPSHPD-   147

                                        173     178
ANABAE: --LPGMEYGITSNEIFHLKTQPKHIAIIGSGYIGTEFAGIMRGLGSQVTQ   194
HUMAN : SQIPGASLGITSDGFFQLEELPGRSVIVGAGYIAVEMAGILSALGSKTSL   215
ECOLI : --IPGVEYGIDSDGFFALPALPERVAVVGAGYIAVELAGVINGLGAKTHL   195
                                    NAD(P)H motif

          197     203
ANABAE: ITRGDKILKGFDEDIRTEIQEGMTNHGIRIIPKNVVTAIQQVPEGLKISL   244
HUMAN : MIRHDKVLRSFDSMISTNCTEELENAGVEVLKFSQVKEVKKTLS--GLEV   263
ECOLI : FVRKHAPLRSFDPMISETLVEVMNAEGPQLHTNAIPKAVVKNTDG-SLTL   244
         2'-P interaction

                                                      282
ANABAE: SGE--------DQEPII-ADVFLVATGRVPNVDGLGLENAGVDVVDSSIE   285
HUMAN : SMVTAVPGRLPVMTMIPDVDCLLWAIGRVPNTKDLSLNKLGIQTDD----   309
ECOLI : ELE--------DGRSET-VDCLIWAIGREPANDNINLEAAGVKTNE----   281
                                                     Loop

          291
ANABAE: GPGYSTMNAIAVNEYSQTSQPNIYAVGDVTDRLNLTPVAIGEGRAFADSE   335
HUMAN : ------KGHIIVDEFQNTNVKGIYAVGDVCGKALLTPVAIAAGRKLAHRL   353
ECOLI : ------KGYIVVDKYQNTNIEGIYAVGDNTGAVELTPVAVAAGRRLSERL   325
        insert

ANABAE: FGNN-LREFSHETIATAVFSNPQASTLGLTEAEARAKHG-DDAVTIYAPF   383
HUMAN : FEYKEDSKLDYNNIPTVVFSHPPIGTVGLTEDEAIHKYGIENVKTYSTSF   403
ECOLI : FNNKPDEHLDYSNIPTVVFSHPPIGTVGLTEPQAREQYGDDQVKVYKSSF   375

ANABAE: RPMYHSFTGKQERIMMKLVVDTKTDKVLGAHMVGENAAEIIQGVAIAVKM   433
HUMAN : TPMYHAVTKRKTKCVMKMVCANKEEKVVGIHMQGLGCDEMLQGFAVAVKM   453
ECOLI : TAMYTAVTTHRQPCRMKLVCVGSEEKIVGIHGIGFGMDEMLQGFAVALKM   425

                    447
ANABAE: GATKKDFDATVGIHPSSAEEFVTMR                           458
HUMAN : GATKADFDNTVAIHPTSSEELVTLR                           478
ECOLI : GATKKDFDNTVAIHPTAAEEFVTMR                           450
```

FIGURE 2: Alignment of primary structures of *Anabaena* (*5*), human, and *E. coli* glutathione reductase. Numbering of human glutathione reductase is based on ref *3*, *E. coli* numbering is from ref *35*. Residues of direct importance for the catalytic function are marked.

culture, equivalent to that of the wild-type enzyme. The expression level of the Δloop mutant was approximately 5 mg/L.

Affinity for Immobilized 2′,5′-ADP−Sepharose. In contrast to the wild-type enzyme, the purified Δloop mutant was shown to bind to 2′,5′-ADP-Sepharose 4B and was eluted with 0.5 M KCl, as was the glutathione reductase from yeast. However, the K203R mutant enzyme did not show any affinity for the gel but was collected in the void volume of the column like the wild-type *Anabaena* enzyme.

Steady-State Kinetics. To determine the optimal conditions for steady-state kinetics, the activity with NADPH and NADH was determined as a function of pH at constant GSSG concentration (Figure 5). With NADPH, the activity was highest at pH 7.0, showing a clear optimum (Figure 5a). In contrast, with NADH the activity increased with increasing pH up to approximately 8.0, and had similar activity as high up as pH 9.3 (Figure 5b), higher than the optimal pH for glutathione reductase from other sources (*7*, *26*, *27*). The steady-state kinetic parameters were determined at the

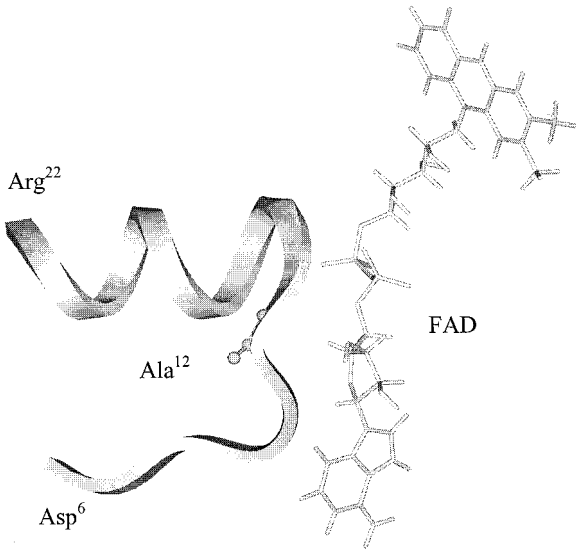

FIGURE 3: FAD site of glutathione reductase. Display of amino acids 6−22 of *Anabaena* structure and the FAD molecule from the superimposed human structure (*12*).

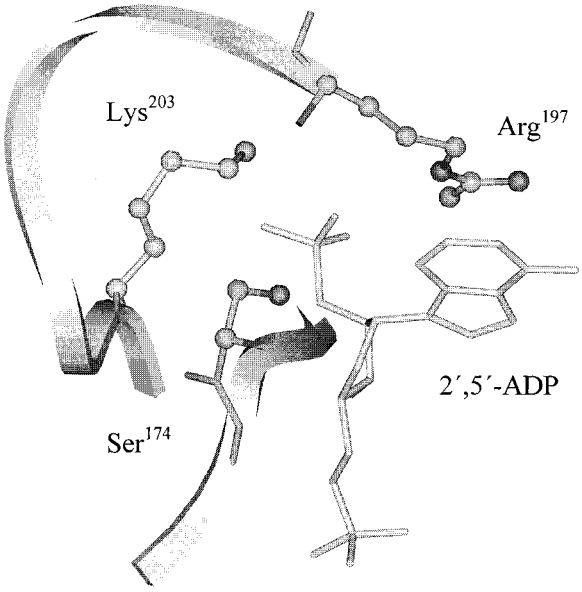

FIGURE 4: Pyridine-nucleotide binding site of glutathione reductase from *Anabaena*, including Ser[174], Arg[197], and Lys[203]. 2′,5′-ADP from the superimposed human structure is modeled into the site.

optimal pH for the two alternative pyridine nucleotides and the kinetic data were analyzed using the rate equation for a ping−pong mechanism (*28*) (Table 1).

At pH 7.0 and 30 °C, the catalytic efficiency of the wild-type enzyme was approximately 48-fold greater with NADPH than with NADH, as a result of both higher k_{cat} and lower K_M (Table 1). The ratio was only marginally reduced, to 44, when the activity with NADH was measured at its optimal pH (8.0). The higher catalytic efficiency with NADH at pH 8.0 than at 7.0 was due to a slightly greater effect on k_{cat} than on K_M. A decreased ratio (39) between the catalytic efficiencies with the two coenzymes was observed at 5 °C.

Introduction of the proposed 2′-phosphate binding residue arginine, instead of the lysine in position 203 resulted in an enzyme (K203R) with lower relative preference for NADPH than that of the wild-type at 30 °C (31-fold). Under these

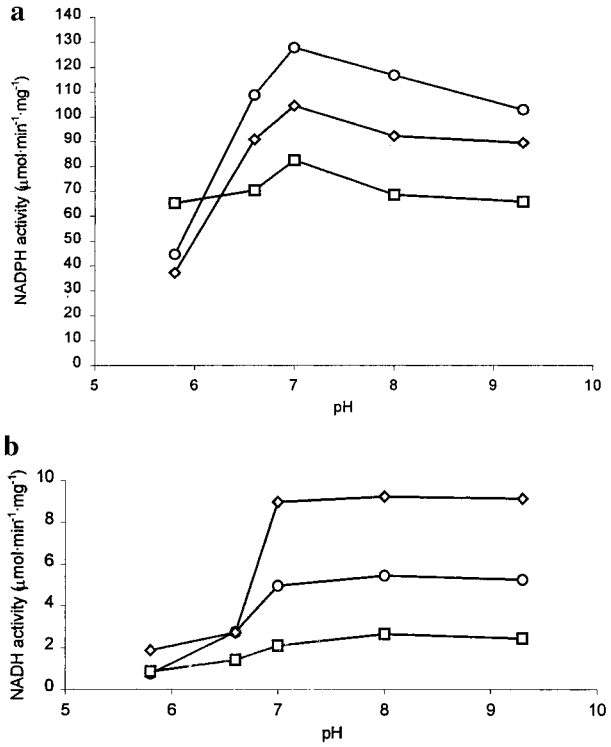

FIGURE 5: pH dependence of wild-type *Anabaena* glutathione reductase. The rate of oxidation of NAD(P)H at 30 °C in buffer containing 1.2 mM GSSG, was measured by monitoring the decrease in absorbance at 340 nm using (a) 200 μM NADPH or (b) 240 μM NADH in 20 mM Na_2HPO_4/NaH_2PO_4 (pH 5.8, 7.0, and 8.0) or Tris-HCl (pH 9.3). Wild-type (○), K203R (□), Δloop (◇).

conditions, the K203R mutant exhibited lower catalytic efficiency with both coenzymes than the wild-type enzyme. In contrast, at 5 °C, the catalytic efficiency with NADPH was higher for the K203R mutant than for the wild-type enzyme (NADH not measured).

By removing the loop, only present in the *Anabaena* glutathione reductase, the enzyme became more efficient with both NADPH and NADH. The relative preference for NADPH was similar to that for the wild-type enzyme. With NADPH, k_{cat} was only marginally affected, while the K_M value decreased 5-fold. In contrast, with NADH, the k_{cat} value increased almost 6-fold, while the K_M value was similar to that for the wild-type enzyme. The overall effect is that the deletion mutant has the highest catalytic efficiency (k_{cat}/K_M) of the three enzyme variants studied, with both coenzymes used.

Preequilibrium Kinetics. The binding of coenzyme and reduction of the enzyme-bound FAD, i.e., the first half-reaction of GSSG reduction was studied under preequilibrium conditions. The rate of formation of an FAD·NAD(P)H charge-transfer complex, as a function of coenzyme concentration, was recorded at 460 nm (Figure 6), while the complete reductive half-reaction (formation of the FAD·thiolate charge-transfer complex) was monitored at 525 nm (Figure 7). The reaction was studied at 5 °C since it was too fast to be measured at 30 °C.

In the reductive half-reaction, the two mutant enzyme forms studied were both more efficient with NADPH than the wild-type enzyme and the Δloop mutant was more efficient with NADH than the wild-type enzyme (Table 2).

Table 1: Steady-state Kinetic Parameters of *Anabaena* Glutathione Reductase

			wild-type		K203R mutant		Δloop mutant	
	pH	temp (°C)	NADPH	NADH	NADPH	NADH	NADPH	NADH
k_{cat} (s^{-1})	7.0	5	22 ± 3	NS[a]	100 ± 18		43 ± 4	
		30	370 ± 10	21 ± 2	250 ± 11	6.0 ± 0.3	300 ± 2	120 ± 40
	8.0	30		38 ± 4		12 ± 1		140 ± 60
K_M (mM)	7.0	5	0.15 ± 0.02	NS[a]	0.38 ± 0.08		0.047 ± 0.005	
		30	0.24 ± 0.01	0.68 ± 0.12	0.38 ± 0.02	0.43 ± 0.05	0.053 ± 0.015	0.82 ± 0.40
	8.0	30		1.1 ± 0.2		0.81 ± 0.01		1.2 ± 0.7
k_{cat}/K_M (mM^{-1} s^{-1})	7.0	5	150	3.7	270		930	
		30	1500	31	430	14	5700	140
	8.0	30		34		15		120
K_M^{GSSG} (μM)	7.0	5	60 ± 10	NS[a]	230 ± 44		130 ± 14	
		30	156 ± 20		211 ± 47		150 ± 13	

[a] NS, not saturated with pyridine nucleotide.

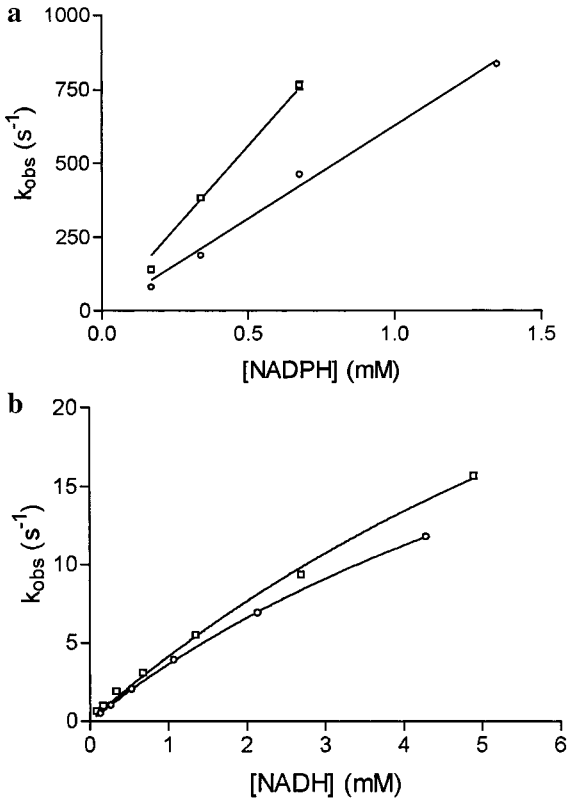

FIGURE 6: Pre-steady-state formation of NAD(P)H·FAD charge-transfer complex of *Anabaena* glutathione reductase variants at 5 °C. The process was monitored at 460 nm in a stopped-flow spectrophotometer. Wild-type (○), K203R mutant (□). (a) k_{obs} vs NADPH (b) k_{obs} vs NADH.

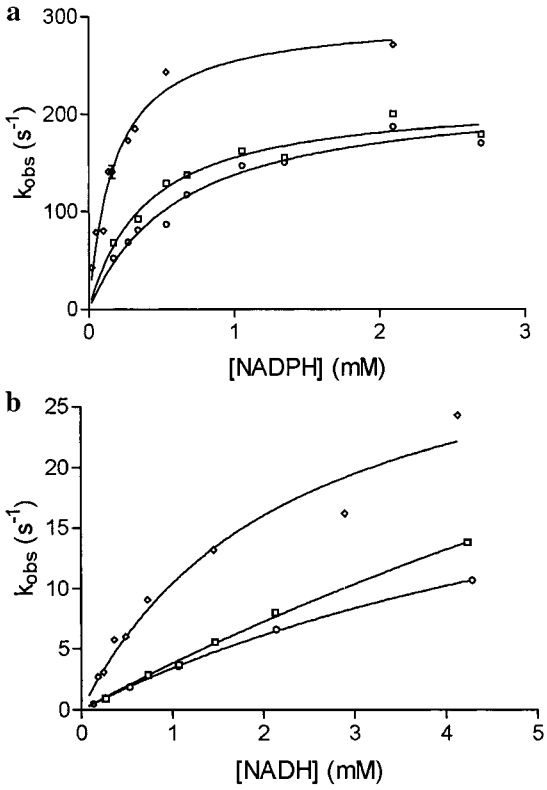

FIGURE 7: Pre-steady-state formation of two-electron reduced enzyme at 5 °C. The reaction was monitored at 525 nm in a stopped-flow spectrophotometer. Wild-type (○), K203R mutant (□), Δloop mutant (◇). (a) k_{obs} vs NADPH (b) k_{obs} vs NADH.

For both mutants, the increased efficiency with NADPH was caused by a reduction of $K_{0.5}$ and for the Δloop mutant there was also an increase of k_{obs}^{max}.

To evaluate if the preference for NADPH as coenzyme was observed also in the reductive half-reaction, the values for $k_{obs}^{max}/K_{0.5}$ (equivalent to k_{cat}/K_M, catalytic efficiency) were determined for both pyridine nucleotides under pre-equilibrium conditions at 460 and 525 nm at 5 °C (Table 2). At 460 nm, the preference of the wild-type enzyme for NADPH was 150-fold, while at 525 nm, the preference was 90-fold, supporting the conclusion that the enzyme is specific for NADPH in both steps of the reductive half-reaction studied. The specificity for NADPH was higher for the K203R mutant in the reductive half-reaction (240-fold at 460 nm and to 140-fold at 525 nm). The Δloop mutant showed a 4-fold higher $k_{obs}^{max}/K_{0.5}$ than the wild-type enzyme with both pyridine nucleotides in the reductive half-reaction. However, the specificity for NADPH over NADH was similar (110-fold at 525 nm). Although the k_{obs}^{max} and $K_{0.5}$ values for NADH were unreliable with the wild-type enzyme and K203 mutant, the values can be used to estimate relative differences. The estimated $K_{0.5}$ values for all enzyme forms with NADH are at least 10-fold higher than with NADPH (525 nm), as is the case for the Δloop mutant. However, the lower efficiency with NADH is also a result of a lower maximal rate (k_{obs}^{max}).

For the wild-type enzyme with NADPH as coenzyme, the oxidative half-reaction appears to be rate limiting for the complete reaction, since the steady-state turnover number, k_{cat}, at 5 °C (22 s^{-1}) was lower than the corresponding limiting rate constant, k_{obs}^{max}, of the first half-reaction (220

Table 2: Preequilibrium Kinetic Parameters of *Anabaena* Glutathione Reductase at 5 °C[a]

		wild-type		K203R mutant		Δloop mutant	
wavelength	kinetic constant	NADPH	NADH	NADPH	NADH	NADPH	NADH
460 nm	$k_{obs}^{max}/K_{0.5}$ ($mM^{-1}\,s^{-1}$)	630 ± 20	4.0 ± 0.04	1100 ± 50	4.5 ± 0.3	ND[b]	ND[b]
525 nm	$k_{obs}^{max}/K_{0.5}$ ($mM^{-1}\,s^{-1}$)	350 ± 40	3.9 ± 0.07	550 ± 80	4.0 ± 0.2	1700 ± 200	15 ± 3
	k_{obs}^{max} (s^{-1})	220 ± 10	(30 ± 1.3)[c]	220 ± 10	(73 ± 18)[c]	300 ± 20	35 ± 5
	$K_{0.5}$ (mM)	0.64 ± 0.11	(7.9 ± 0.5)[c]	0.40 ± 0.07	(18 ± 5)[c]	0.18 ± 0.03	2.3 ± 0.7

[a] Kinetic parameters were obtained by nonlinear regression analysis of experiments presented as graphs of k_{obs} vs NAD(P)H concentrations (Figures 6 and 7). $k_{obs}^{max}/K_{0.5}$ was determined as the slope of the curve at zero coenzyme concentration, k_{obs}^{max} is the maximal observed rate constant and $K_{0.5}$ is the concentration of pyridine nucleotide resulting in half the maximal observed enzymatic rate. [b] ND, not determined. [c] Values in parentheses are approximate due to lack of saturation with NADH under the experimental conditions used.

s^{-1}). The corresponding analysis could not be performed with NADH due to lack of saturation (Figure 7).

DISCUSSION

Alignment and Structural Model. Algorithms that align sequences and analyze their similarities are mathematical tools that make it possible to compare proteins and to predict the properties of uncharacterized structures. The algorithms are based on certain assumptions and simplifications, and although the reliability increases with the degree of similarity for the proteins compared, the predictions should be used with caution. The glutathione reductase sequences of human and *E. coli* were aligned differently when matched with primary structures from eight other species than when the two three-dimensional structures were superpositioned. Since the sequence of the *Anabaena* enzyme was similar to both the enzyme from human and *E. coli*, it was necessary to use both of the available glutathione reductase structures for modeling and employ the sequence alignment to determine which structure to use for different regions. The most difficult regions to model were obviously those with limited sequence identity and where gaps had to be inserted. The most divergent part is the region of the interface between the two subunits, residues 52−79, where the length of the polypeptide chain varies and no conservation in the sequence can be observed. It was shown in several positions that gaps should not be placed adjacent to each other, but might be separated by one or several residues.

Structure and Functional Importance of Unique Anabaena Loop. Human and *Anabaena* glutathione reductase both contain a loop close to the entrance of the coenzyme-binding site, although they are positioned on opposite sides of the cleft. The exact position and conformation of the loop residues present only in the *Anabaena* enzyme could not be determined. It is possible that it is quite flexible, since if it were tightly associated with the NAD(P)H site it would hinder the entrance of NAD(P)H and exit of $NAD(P)^+$. Experimental determination of the structure of *Anabaena* glutathione reductase will reveal the accuracy of the present model.

The loop in the *Anabaena* enzyme was demonstrated to affect the catalytic properties of the enzyme. Initially, it was found that the loop influenced the interaction of the enzyme with immobilized 2′,5′-ADP. It had previously been found that the wild-type enzyme did not bind to 2′,5′-ADP-Sepharose 4B, and the structural model indicated that the loop might sterically hinder the binding of the enzyme to the affinity matrix. Removal of the loop did indeed make it possible for the protein to bind to this affinity gel, and it appears that the NAD(P)H-binding site in the Δloop mutant has become more exposed, allowing interaction with the affinity ligand.

Similarly, removal of the loop increased the catalytic efficiency of the enzyme, with NADPH by reducing K_M and with NADH by increasing k_{cat}. Rapid kinetic studies with the loop mutant also demonstrated decreased half-saturation concentrations and higher catalytic efficiencies, with both NADPH and NADH, in the reductive half-reaction. Since the loop is not part of the active site, it modifies the catalytic properties of the enzyme in an indirect manner. This appears to be an example of a region where relatively large structural variations can be introduced and the properties of the enzyme can be changed in a subtle manner. Removal of the loop changed the relatively low activity of the *Anabaena* enzyme into a more efficient form of glutathione reductase.

Catalytic Properties of Anabaena Glutathione Reductase. Steady-state kinetic data showed that *Anabaena* glutathione reductase was active with both NADH and NADPH. The wild-type enzyme from *Anabaena* has a higher k_{cat} with NADPH than both the human (*27*) and the *E. coli* enzymes (*7*). However, the K_M is higher for NADPH as compared with the corresponding values of the *E. coli* and human enzyme (*6*). The net effect with NADPH is that the catalytic efficiency of *Anabaena* glutathione reductase (k_{cat}/K_M) is lower.

The pH optimum for wild-type *Anabaena* enzyme is 7 with NADPH and 8 with NADH (Figure 5). In contrast, the optimal pH values with NADH are 4.7 for the *E. coli* enzyme and 5.7 for the enzyme from human erythrocytes (*7, 26, 29*).

Affinity and Specificity for Pyridine Nucleotide. It was of interest to find out if the *Anabaena* enzyme would be more efficient with NADH than with NADPH. The NAD(P)H-binding motif (173−178) in the *Anabaena* sequence differs from the glutathione reductase consensus of G-(A/G)-G−Y-I-A, having glycine in the C-terminal position (Gly^{178}), a motif typical of NADH-dependent enzymes. In addition, glutathione reductase from other sources has two conserved arginines, of which one is replaced by lysine in the *Anabaena* enzyme. It was speculated that the arginine was important for coenzyme specificity since it has been shown to interact with the 2′-phosphate of NADPH in the known glutathione reductase structures.

The catalytic efficiency for wild-type *Anabaena* glutathione reductase was 45-fold lower with NADH than with NADPH, an effect of both lower k_{cat} and higher K_M. The catalytic efficiency of glutathione reductase from other sources is more strongly in favor of NADPH over NADH. The ratios of the corresponding k_{cat}/K_M values for the two

pyridine nucleotides of the enzyme from *E. coli* (64 000), yeast (1800), human (490), and spinach (540) (*26*, *27*, *30*) suggest that in these biological species the contribution of NADH to cellular GSSG reduction is negligible.

To improve the efficiency of the *Anabaena* enzyme with NADPH, the K203R mutant was designed. Surprisingly, the K203R mutant did not bind to 2′,5′-ADP-Sepharose 4B. In addition, the K_M value for NADH decreased, while the K_M value for NADPH increased, in contrast to what was predicted. These results indicate that this single change was not sufficient to improve the affinity for the immobilized 2′,5′-ADP or the specificity for NADPH and that the presence of lysine in position 203 instead of arginine was not a primary determinant for specificity. Glutathione reductase from *Onchocerca volvulus* (*31*) was also more active with NADPH than with NADH, despite the presence of Trp in the position corresponding to *Anabaena* Lys^{203}. This confirms that the preference for NADPH is possible despite lack of a second arginine linked to the 2′-phosphate of NADPH.

Mutagenesis studies of *E. coli* glutathione reductase have previously shown that replacement of Ala^{179} by Gly resulted in a dramatic decrease in K_M for NADH (*7*). Although the value was almost 40-fold lower than for the wild-type enzyme and of the same order as the K_M for NADPH, the coenzyme specificity did not change. Several additional mutations are required to obtain a high k_{cat} value and to change the coenzyme specificity. To drastically decrease the affinity for NADP(H), a negatively charged residue in the binding site must be introduced. The A179G replacement in the *E. coli* enzyme changed the structure of the NADP/NAD-binding site, which facilitated direct interaction between the negatively charged residue and the 2′ and 3′-hydroxyl groups of the AMP moiety of NADH (*32*). In the case of the *Anabaena* enzyme, the pyridine-nucleotide-binding site does not contain the negatively charged residue in the relevant position, and this mechanism for discriminating against NADPH is ruled out.

Finally, modeling revealed that, in *Anabaena* glutathione reductase, the 2′-phosphate of NADPH might form a hydrogen bond with Ser^{174}, in the coenzyme-binding motif (Figure 4). Glutathione reductase from other sources has glycine or alanine instead of serine in this position. The presence of serine is hypothesized to be sterically acceptable when the otherwise conserved arginine is replaced by the smaller lysine. The energy in forming the hydrogen bond between the 2'-phosphate of NADPH with Ser^{174} is thought to be different from that due to forming an ion−ion interaction with Arg^{203}. Thus, two different modes of interactions with the coenzyme appear to exist, both adequate for activity, but resulting in slightly different enzymatic characteristics.

Reductive Half-Reaction and Rate-Determining Kinetic Steps. Preequilibrium studies revealed distinct kinetic differences between the engineered mutants and the wild-type enzyme. The reductive half-reaction can be resolved into three spectrophotometrically distinguishable steps (*33*). The first rapid step involves formation of a charge-transfer complex between pyridine nucleotide and oxidized enzyme-bound FAD (binding of coenzyme) and is visible as a partial bleaching of the flavin absorbance peak at 460 nm. Second, reduced absorbance at shorter wavelengths (420 nm) represents the breaking of the hydrogen bond with the nucleotide (oxidation of coenzyme and reduction of enzyme), identified by a kinetic isotope effect (*33*). Finally, formation of the two-electron reduced enzyme appears as increased absorbance at 530 nm (*19*). As discussed above, the *Anabaena* enzyme had a k_{cat} higher than the enzyme from other sources. Similarly, the maximal k_{obs} is 220 s^{-1} for the *Anabaena* enzyme in the reductive half-reaction with NADPH is high in comparison to the enzyme from other sources studied, being 110 s^{-1} at 4 °C (independent of the NADPH concentration) for the *E. coli* enzyme (monitored at 525) (*34*) and 68 s^{-1} (at 5 °C) for the yeast enzyme (monitored at 530 nm) (*33*). However, the k_{cat} from steady-state kinetics for the wild-type *Anabaena* enzyme (22 s^{-1}) at 5 °C is 1 order of magnitude lower than the maximal rate of the first half-reaction (220 s^{-1}) with NADPH, indicating that the rate-limiting step is in the oxidative half-reaction.

Although substitution of Lys^{203} with Arg increased the k_{cat} of the steady-state reaction at 5 °C, it did not change the maximal rate with NADPH in the reductive half-reaction (at the same temperature). The increased "efficiency" observed at 460 (1.7-fold) and at 525 nm (1.6-fold) is therefore attributed to a decrease in the $K_{0.5}$ for NADPH. Under steady-state conditions, the increase was less (1.2-fold). Since the effect becomes smaller as the reaction proceeds, it appears that it is caused by an early step in the reaction mechanism. Removal of the loop resulted in a dramatic increase of the efficiency in the reductive half-reaction with both NADPH and NADH, primarily as a result of a decreased $K_{0.5}$, although the k_{obs}^{max} also increased somewhat with NADPH.

Also, the specificity for the pyridine nucleotide was not altered in any of the enzyme variants studied, in either the first half-reaction or the complete reaction. It appears that the more efficient reaction with NADPH is due to more favorable interactions with the enzyme, although they cannot simply be attributed to the nature of individual residues, e.g., the exact sequence of the pyridine-nucleotide-binding motif. It is the combination of different amino acids in key positions that determine the catalytic efficiency of the enzyme with both coenzymes.

Since removal of the loop had the greatest effect on catalysis, resulting in the most efficient enzyme form studied, it appears that the loop is of functional importance for the *Anabaena* enzyme. It is not evident why the native enzyme form has this extra sequence as it reduces the activity of the enzyme. Unless it adds unrecognized additional functionality to the enzyme it would appear that there has not been evolutionary pressure to improve the efficiency of the enzyme to the same level as the enzyme from other sources. Nevertheless, the present results show that a more efficient catalyst can be designed by a simple sequence deletion.

ACKNOWLEDGMENT

We thank Prof. Georg Schulz, University of Freiburg, for providing the coordinates of the *E. coli* glutathione reductase structure and Prof. Richard N. Perham, University of Cambridge, for the *E. coli* strain SG5. The students of "Biochemical Methodology, MB1" in the autumn course 1998 provided preliminary affinity chromatography data of importance. This work is part of a collaboration with Professor Birgitta Bergman, Department of Plant Physiology, Stockholm University, who kindly supported the project.

REFERENCES

1. Williams, C. H., Jr. (1992) in *Chemistry and Biochemistry of Flavoenzymes* (Müller, F, Ed.) pp 121−211, CRC Press, Boca Raton.
2. Schirmer, R. H., Krauth-Siegel, R. L., and Schulz, G. E. (1989) in *Coenzymes and Cofactors* (Dolphin, D., Poulson, R., and Avramovic, O, Ed.) Vol. 3A, pp 553−596, Wiley, New York.
3. Karplus, P. A., and Schulz, G. E. (1987) *J. Mol. Biol. 195*, 701−729.
4. Mittl, P. R. E., and Schulz, G. E. (1994) *Protein Sci. 3*, 799−809.
5. Jiang, F., Hellman, U., Sroga, G. E., Bergman, B., and Mannervik, B. (1995) *J. Biol. Chem. 270*, 22882−22889.
6. Jiang, F., and Mannervik, B. (1999) *Protein Expression Purif. 15*, 92−98.
7. Scrutton, N. S., Berry, A., and Perham, R. N. (1990) *Nature 343*, 38−43.
8. Rescigno, M., and Perham, R. N. (1994) *Biochemistry 33*, 5721−5727.
9. Pai, E. F., Karplus, P. A., and Schulz, G. E. (1988) *Biochemistry 27*, 4465−4474.
10. Mannervik, B., Jacobsson, K., and Boggaram, V. (1976) *FEBS Lett. 66*, 221−224.
11. Connell, J. P., and Mullet, J. E. (1986) *Plant Physiol. 82*, 351−356.
12. Karplus, P. A., and Schulz, G. E. (1989) *J. Mol. Biol. 210*, 163−180.
13. Abola, E. E., Bernstein, F. C., Bryant, S. H., Koetzle, T. F., and Weng, J. (1987) in *Crystallographic databases: Information, content, software systems, scientific applications* (Allen, F. H., Bergerhoff, G., and Sievers, R, Ed.) pp 107−132, Data Commission of the International Union of Crystallography, Bonn.
14. Bernstein, F. C., Koetzle, T. F., Williams, E. F., Meyer, E. E. Jr., Brice, M. D., Rodgers, J. R., Kennard, O., Shimanouchi, T., and Tasumi, M. (1977) *J. Mol. Biol. 112*, 535−542.
15. Higuchi, R., Krummel, B., and Saiki, R. K. (1988) *Nucleic Acids Res. 16*, 7351−7367.
16. Widersten, M., and Mannervik, B. (1995) *J. Mol. Biol. 250*, 115−122.
17. Sanger, F., Nicklen, S., and Coulson, A. R. (1977) *Proc. Natl. Acad. Sci. U.S.A. 74*, 5463−5467.
18. Blum, H., Beier, H., and Gross, H. J. (1987) *Electrophoresis 8*, 93−99.
19. Massey, V., and Williams, C. H., Jr. (1965) *J. Biol. Chem. 240*, 4470−4480.
20. Carlberg, I., and Mannervik, B. (1981) *Anal. Biochem. 116*, 531−536.
21. Bulger, J. E., and Brandt, K. G. (1971) *J. Biol. Chem. 246*, 5510−5577.
22. Boggaram, V., and Mannervik, B. (1978) *Biochem. Biophys. Res. Commun. 83*, 558−564.
23. Berry, A., Scrutton, N. S., and Perham, R. N. (1989) *Biochemistry 28*, 1264−1269.
24. Wong, K. K., Vanoni, M. A., and Blanchard, J. S. (1988) *Biochemistry 27*, 7091−7096.
25. Krauth-Siegel, R. L., Arscott, L. D., Schönleben-Janas, A., Schirmer, R. H., and Williams, C. H., Jr. (1998) *Biochemistry 37*, 13968−13977.
26. Worthington, D. J., and Rosemeyer, M. A. (1976) *Eur. J. Biochem. 67*, 231−238.
27. Scott, E. M., Duncan, I. W., and Ekstrand, V. (1963) *J. Biol. Chem. 238*, 3928−3933.
28. Mannervik, B., Boggaram, V., Carlberg, I., and Larson, K. (1980) in *Flavins and Flavoproteins* (Yagi, K., and Yamano, T, Ed.) pp 173-187, Japan Scientific Societies Press, Tokyo.
29. Icén, A. (1967) *Scand. J. Clin. Lab. Invest.* (Suppl.) *96*, 36.
30. Vanoni, M. A., Wong, K. K., Ballou, D. P., and Blanchard, J. S. (1990) *Biochemistry 29*, 5790−5796.
31. Müller, S., Gilberger, T., Fairlamb, A. H., and Walter, R. D. (1997) *Biochem. J. 325*, 645−651.
32. Mittl, P. R. E., Berry, A., Scrutton, N. S., Perham, R. N., and Schulz, G. E. (1993) *J. Mol. Biol. 231*, 191−195.
33. Huber, P. W., and Brandt, K. G. (1980) *Biochemistry 19*, 4568−4575.
34. Rietveld, P., Arscott, D., Berry, A., Scrutton, N. S., Deonarain, M. P., Perham, R. N., and Williams, C. H., Jr. (1994) *Biochemistry 33*, 13888−13895.
35. Greer, S., and Perham, R. N. (1986) *Biochemistry 25*, 2736−2742.

BI9903300